JUNE 15, 1934 PHYSICAL REVIEW VOLUME 45

The Band Spectrum of Ionized Aluminum Hydride[1]

G. M. ALMY AND M. C. WATSON, *Laboratory of Physics, University of Illinois*

(Received April 25, 1934)

The Schüler hollow aluminum cathode lamp, containing helium and hydrogen, maintained at 2000 volts d.c., has been used to excite the band spectrum of AlH, which has been photographed with a 21-foot grating spectrograph. Among the new systems appearing there is one with principal head at 3632A which on analysis proves to consist of the (0,0) and (1,1) bands of a $^2\Pi$ (regular)$\rightarrow {}^2\Sigma^+$ system due to AlH$^+$. The $^2\Pi$ state is found to be regular and not inverted as suggested by Holst. The various band constants are obtained and the spin and Λ-doubling compared with theory.

INTRODUCTION

THE band spectrum of AlH has been studied extensively, chiefly by the spectroscopists at Stockholm, using in most cases the Al arc in hydrogen as source. As a preliminary experiment in the use of the hollow cathode lamp of the Schüler type as a source for the excitation of molecular spectra we have photographed the spectrum of AlH. All of the known bands of AlH have been excited with good intensity in this source, as well as several new systems in the ultraviolet, which, however, have also been recently photographed by Holst.[2, 3] Holst has recently reported[3] briefly the results of his analysis of a band at 3632A finding it to be a $^2\Pi$ (inverted)$\rightarrow {}^2\Sigma$ transition in AlH$^+$ with a coupling constant (A) in the $^2\Pi$ state equal to -39 cm^{-1}. When we discovered this announcement we had just completed an analysis of this system with quite different results. The purpose of this paper is to present our analysis which we believe to be the correct one.

EXPERIMENTAL METHOD

The hollow cathode lamp is of the type described by Schüler,[4] built and placed in a gas-circulating system according to suggestions from Professor Kruger of this laboratory. The discharge, maintained at 2000 volts d.c. by a four-tube hot-cathode mercury rectifier, was carried principally by helium at a few mm pressure to which a small amount of hydrogen was occasionally added. The gas was circulated by a mercury pump; charcoal and chabasite traps were used to remove undesirable gaseous impurities. The intensity of the hydride spectra increased with increasing amounts of hydrogen, but if too much were used the many-lined and continuous spectra of H_2 obscured the *spectra* of the hydride. The proper amount of H_2 and the best pressure of He to give intense hydride spectra without too much background were determined by trial.

This source has several advantages over the low pressure arc: (1) only a little of the element whose hydride is being examined is needed, (2) the metal cathode can be immersed in water, or in liquid air, to reduce the Doppler effect, (3) molecular-ion spectra are probably produced with greater intensity, (4) the source can be operated for hours with little attention.

After preliminary photographs with a Hilger E1 quartz spectrograph the final plates of the bands at 3632A were taken in the first order of a 21-foot grating, 30,000 lines per inch, dispersion 1.3A per mm. Wave-number measurements on one-hour and eight-hour exposures showed excellent agreement. The wave numbers (in vacuum) listed in Table I were calculated from the measurements (mean of two observers) on the eight-hour plate, a reproduction of which appears in Fig. 1.

---

[1] Paper presented at Washington meeting of American Physical Society, April 27, 1934. Cf. Bulletin **9**, No. 2, p. 20, April 10, 1934.

[2] W. Holst, Nature **132**, 207 (1933); Zeits. f. Physik **86**, 338 (1933).

[3] W. Holst, Nature **132**, 1003 (1933).

[4] H. Schüler, Zeits. f. Physik **59**, 149 (1929).

TABLE I. *Wave numbers arranged in branches.*

For P_1, Q_1 and R_1, $J''=K''+\frac{1}{2}$; for P_2, Q_2 and R_2, $J''=K''-\frac{1}{2}$. Asterisk indicates superposition. *d* = diffuse, *dv* = diffuse to violet, *dr* = diffuse to red.

				(0,0) band				
K''	I	$^PQ_{12}$	I	P_1	I	Q_1	I	R_1
0					3	27,672.50	0	27,691.25
1			3	27,659.30	8	678.16	7*dv*	709.08*
2			5	651.87	6	683.14	2*d*	727.29
3			6	643.88	6	687.84	5*d*	744.85*
4			6	635.49	6*dv*	692.28*	7	761.76*
5			10*d*	626.73*	8	696.42	3	778.80*
6			9*d*	618.10	8	700.58	10*dr*	795.87*
7			8*d*	609.34	7	704.72	5	812.89*
8			8	600.64	7*dv*	709.08*	4	830.11
9	1	27,592.70	8	592.06	7	713.35	6*d*	847.33*
10	1	584.44	8	583.88	6	717.89	2	864.59*
11	1	576.60	8	575.92	6	722.72	3	882.19
12	1	569.10	6	568.38	3	727.84	5	899.81*
13	0	561.96	6	561.25	6	733.26	2	917.78
14	0	555.37	5	554.58	5	739.01	4	936.03*
15			10*dv*	548.48*	4*d*	744.85*	2*d*	954.32
16			4*d*	542.75	5	751.76	4*d*	973.26*
17			3	537.76	3	758.73	2	991.77*
18			3	533.39	5*d*	766.26*	1	28,011.11
19			4*d*	529.52	1	774.26*	1	030.67
20			2	526.92	2	782.96	1	050.82
21			2*d*	524.43	3	792.20*	3	071.01
22			3*d*	523.14	2	802.03	2*dv*	091.40*
23			3*d*	523.14	5	812.89*	2*d*	113.03
24			1	525.17			2*d*	134.75
25			0	528.05			1	156.53
26								

		(1,1) band				
K''	I	P_1	I	Q_1	I	R_1
0			2*d*	27,824.02	2	27,842.19
1	3	27,811.49	2	829.48	3	859.94*
2	2	805.09	4	835.11	1	877.87
3	3*d*	798.30	3	840.63	1	895.58
4	3*d*	791.44	5	846.12	2	913.45
5	10*dv*	785.02*	5	851.55*	2	931.56
6	4	778.80*	5	857.43	4	949.77
7	4*d*	771.99*	3	863.55	3	968.35
8	5*d*	766.26*	15	869.97	5*d*	987.56*
9	2	760.50	2	877.16	4	28,006.56*
10	2	755.79	3	884.65	2	026.43
11	5	751.76*	3	892.84	2	046.82
12	2	748.27*	6*d*	901.92*	3*d*	067.58*
13	3	745.83*	3	911.29	2*d*	089.17
14			2	921.58	3*dr*	111.32*
15			1	932.80	1*d*	134.08
16			5	944.97*		
17			2*d*	958.17		
18			1*d*	972.48		
19			5*d*	987.56*		
20			4*d*	28,002.85*		

K''	I	P_2	I	Q_2	I	R_2
0						
1					1	27,774.26*
2			2	27,748.27	9	785.02*
3	7*dv*	27,709.08*	3	745.83*	10*dr*	795.87*
4	6*dv*	692.28*	4*d*	743.41*	6*d*	807.59
5	2	677.06	8*d*	742.03	6	820.11
6	2	663.43	8*d*	742.03	5*d*	833.36
7	4	650.64	8*d*	742.03	6*d*	847.33*
8	3	638.22	4*d*	743.41*	4	861.64
9	10*d*	626.73*	5*d*	744.85*	2	876.58
10	6	615.51	5	747.05	2*d*	891.95
11	5	605.30	4	749.86	3	907.73
12	5	595.73	4	753.29	2	923.98
13	4	586.85	5	757.23	2	940.45
14	4	578.65	8	761.76*	2*d*	957.51
15	3	571.16	5*d*	766.26*	2*dv*	974.82
16	4*d*	564.42	4*d*	771.99*	2	992.42
17	2*dr*	558.27	4*d*	778.12	1*d*	28,010.67
18	3	552.94	9	785.02*	1	029.02
19	10*dv*	548.48*	3	792.20*	2	048.00
20	2*d*	544.73	3	800.21	3*d*	067.58*
21	1*d*	541.88	1	808.84	4*d*	087.10
22	3	539.89	3*d*	818.30	3	107.14
23	3	538.82*	1	828.43	1*d*	127.98
24	3	538.82*	2	839.37	2*d*	148.68
25			5	851.55*	3*d*	169.93
26			2	864.59*		

K''	I	P_2	I	Q_2	I	R_2
0						
1					0	27,925.95
2			6*d*	27,901.92*	2	936.65
3	2	27,864.59*	5	899.81*	4	947.88
4	1	850.24	4*dr*	898.48*	4*d*	960.07
5	1	836.78	4*dr*	898.48*	4*d*	973.26*
6	1	824.68	5	899.81*	5*d*	987.56*
7	1	813.74	6*d*	901.92*	4*d*	28,002.85*
8	3	804.04	4	905.23	3	019.09
9	10*dr*	795.87*	3	909.58	3	036.00
10	2	787.68	3	914.77	5*d*	053.77
11	2	781.19	2	920.99	2	072.31
12	6	775.55	3	927.96	2*dv*	091.40*
13	1*d*	771.35	4	936.03*	3*dr*	111.32*
14	3	767.89	5	944.97*	1	132.13
15	5*d*	766.26*	2	954.94	2	153.74
16			2*d*	966.05	2*d*	175.87
17			2*d*	978.32	3	199.18
18			2	991.77*	1*d*	223.97
19			4	28,006.56*		
20			2*d*	022.48		
21			2	039.74		

ANALYSIS OF SPECTRUM. MOLECULAR CONSTANTS

An analysis of the spectrum showed that practically all of the lines of fair intensity could be formed into two bands of six strong branches each, as shown in the Fortrat diagram (Fig. 2) and in the lists of wave numbers (Table I). These bands are accounted for by assuming them to be the (0,0) and (1,1) bands of a $^2\Pi$ (regular)$\rightarrow{}^2\Sigma^+$ transition. That the $^2\Pi$ state is regular (not inverted, as suggested by Holst) is indicated by the presence of $Q_1(1/2)$ and $P_1(3/2)$ in each band. These lines would be absent if the $^2\Pi$ state were inverted. No other assigned band line is superimposed on any of these four lines. The $^PQ_{12}$ "satellite" branch was resolved from the (0,0) P_1 branch beyond $P_1(9\frac{1}{2})$ but became too faint to observe beyond $P_1(14\frac{1}{2})$. This satellite branch enables one to fix the sign and magnitude of the spin doubling in the $^2\Sigma^+$ state. The origins of the (0,0) and (1,1) bands figured from the first lines in the Q branches are:

for the (0,0) band, $\nu_1=27{,}667.8\text{ cm}^{-1}$ $\nu_2=27{,}760.2\text{ cm}^{-1}$
for the (1,1) band, $\nu_1=27{,}819.5\text{ cm}^{-1}$ $\nu_2=27{,}912.5\text{ cm}^{-1}$.

Since AlH has an even number of electrons its states are singlets and triplets. This band

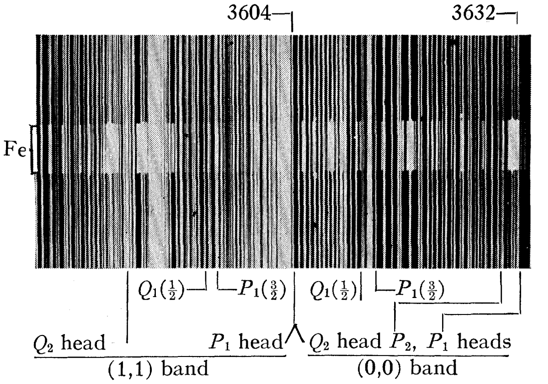

FIG. 1. Part of AlH$^+$ band system ($^2\Pi$(reg)$\rightarrow{}^2\Sigma^+$). The presence of the indicated first lines in P_1 and Q_1 branches requires that the $^2\Pi$ state be regular.

spectrum, therefore, is probably due to AlH$^+$. This assumption is strongly supported by the close similarity of this spectrum to the analogous system in MgH. Since on this assignment the configuration of the $^2\Sigma$ state is $(3s\sigma)^2 3p\sigma$, it may be written $^2\Sigma^+$.

TABLE II. *Term differences.*
$\Delta_2F''(K'') = R(K''-1) - P(K''+1)$.

	(0,0) band:		(1,1) band:	
K''	Δ_2F_1''	Δ_2F_2''	Δ_2F_1''	Δ_2F_2''
0				
1	39.38		37.10	
2	65.20	65.18	61.64	61.36
3	91.80	92.74	86.43	86.41
4	118.47	118.81	110.56	111.10
5	143.66	144.16	134.65	135.39
6	169.46	169.47	159.57	159.52
7	195.23	195.14	183.51	183.52
8	220.83	220.60	207.85	206.98
9	246.23	246.13	231.77	231.41
10	271.41	271.28	254.80	254.81
11	296.21	296.22	278.16	278.22
12	320.94	320.88	300.99	300.96
13	345.23	345.33		323.51
14	369.30	369.29		345.06
15	393.28	393.09		
16	416.56	416.55		
17	439.87	439.48		
18	462.25	462.19		
19	484.19	484.29		
20	506.24	506.12		
21	527.68	527.67		
22	547.87	548.28		
23	566.23	568.32		
24	584.98			

$^2\Sigma^+$ state

In the $^2\Sigma^+$ state, for either the F_1 or F_2 states if one neglects spin doubling,

$$F(K) = B_v(K+\tfrac{1}{2})^2 + D_v(K+\tfrac{1}{2})^4 \cdots$$

$$\Delta_2F(K) = F(K+1) - F(K-1)$$
$$= 4B_v(K+\tfrac{1}{2}) + 8D_v(K+\tfrac{1}{2})^3 \cdots$$

to a high degree of approximation. Values of Δ_2F'' are listed in Table II. Δ_2F_2'' and Δ_2F_1'' are the same to within errors of measurement (due largely to superpositions of lines) and thereby indicate a very small spin doubling in the $^2\Sigma^+$ state. In Fig. 3b the average $\Delta_2F''(K'')/4(K''+\frac{1}{2})$ from F_1 and F_2 states is plotted against $K''+\frac{1}{2}$. The intercept at $K''=-\frac{1}{2}$ is the value of B_v''. B_v'' and D_v'' were also obtained by a least squares calculation using values of $\Delta_2F''/4(K''+\frac{1}{2})$ smoothed to the curves in Fig. 3b. From this calculation:

$$B_0'' = 6.564\ \text{cm}^{-1} \quad D_0'' = -0.000474\ \text{cm}^{-1}$$
$$B_1'' = 6.166\ \text{cm}^{-1} \quad D_1'' = -0.000465\ \text{cm}^{-1}.$$

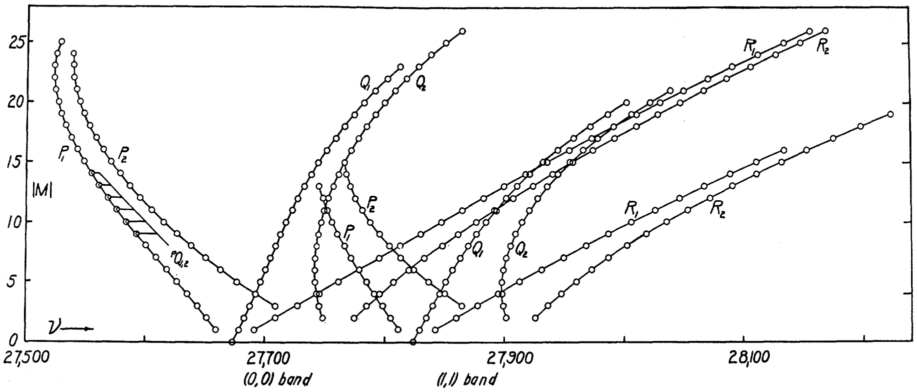

FIG. 2. Fortrat diagram of AlH$^+$ $^2\Pi$(reg)$\rightarrow{}^2\Sigma^+$ band system.

From these one obtains:

$$\alpha''=B_0''-B_1''=0.398\ \text{cm}^{-1}$$
$$r_e''=1.60\text{A}$$
$$B_e''=6.763\ \text{cm}^{-1}$$
$$\omega_e''=(4B_e''^3/-D_e'')^{\frac{1}{2}}=1610\ \text{cm}^{-1}.$$

The $^2\Sigma$ spin doubling was obtained from the $^PQ_{12}$ branch since:

$$\Delta\nu_{12}={}^PQ_{12}(K'')-P_1(K'').$$

According to the theory of spin doubling[5] in $^2\Sigma$ states:

$$\Delta\nu_{12}=\gamma(K''+\tfrac{1}{2})$$

where γ is a constant. In Fig. 4c the observed values of $\Delta\nu_{12}$ are plotted against K''. The straight line is $0.056(K''+\frac{1}{2})$, hence $\gamma=0.056$ cm^{-1}.

$^2\Pi$ state

Since, as will be shown, the Λ-type doubling is very small, we assume that the $^2\Pi$ state follows the Hill and Van Vleck equation. Thus:

$$F(J)=B_v\{(J+\tfrac{1}{2})^2-1\pm\tfrac{1}{2}[Y(Y-4)+4(J+\tfrac{1}{2})^2]^{\frac{1}{2}}\}+D_v(J+\tfrac{1}{2})^4 \tag{1}$$

where $Y=A/B_v$, upper sign (+) for F_2, lower sign for F_1. Hence

$$\frac{\Delta_2F(J)}{4(J+\frac{1}{2})}=B_v\left\{1\pm\frac{[Y(Y-4)+4(J+\frac{3}{2})^2]^{\frac{1}{2}}-[Y(Y-4)+4(J-\frac{1}{2})^2]^{\frac{1}{2}}}{8(J+\frac{1}{2})}\right\}+2D_v(J+\tfrac{1}{2})^2. \tag{2}$$

In Fig. 3a values of $\Delta_2F'(J)/4(J+\frac{1}{2})$ are plotted against $J+\frac{1}{2}$ for the $F_2(^2\Pi_{\frac{3}{2}})$ and $F_1(^2\Pi_{\frac{1}{2}})$ levels. From Eq. (2) it is obvious that the mean of the two curves should be given by $B_v+2D_v(J+\frac{1}{2})^2$. By least squares the following constants were found to fit best the mean curve, using values of $\Delta_2F/4(J+\frac{1}{2})$ for $J>5$, because of the uncertain behavior at small J:

$$B_0'=6.727\ \text{cm}^{-1}\quad D_0'=-0.000414\ \text{cm}^{-1}$$
$$B_1'=6.479\ \text{cm}^{-1}\quad D_1'=-0.000409\ \text{cm}^{-1},$$

whence

$$B_e'=6.851\ \text{cm}^{-1},\quad r_e'=1.58\text{A},\quad \omega_e'=1753\ \text{cm}^{-1}.$$

On account of inaccuracy in D_v' and D_v'', values of ω_e' and ω_e'' computed as described are not very reliable. The difference between origins of the (0,0) and (1,1) bands is, however, equal to $\omega_e'-\omega_e''$ to within a few cm^{-1}.

The computation of B_e' does not depend upon the magnitude of the term to the one-half power in Eq. (1), but only upon the fact that $\Delta_2F_2/4(J+\frac{1}{2})$ and $\Delta_2F_1/4(J+\frac{1}{2})$ are symmetrically above and below $[B_v+2D_v(J+\frac{1}{2})^2]$.

The next step was to choose the best value of A. From Eq. (1):

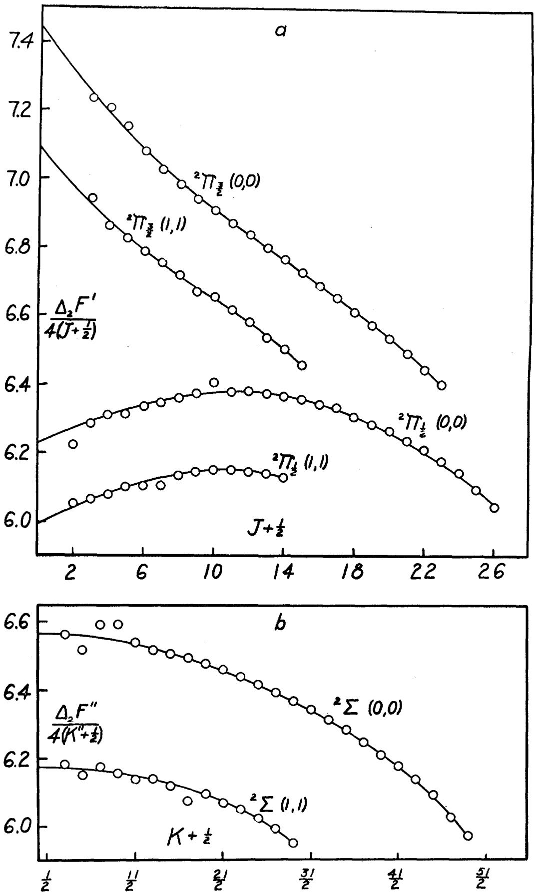

FIG. 3. Values of $\Delta_2F/4(J+\frac{1}{2})$ for all observed states. (a) $^2\Pi$, (b) $^2\Sigma$. Intercepts at left give approximate values of B.

---

[5] The discussion of spin and Λ-type doubling in this paper is based on the account of these effects given in

[a] R. S. Mulliken, Rev. Mod. Phys. **3**, 89–155 (1931).

[b] R. S. Mulliken and A. Christy, Phys. Rev. **38**, 87 (1931).

$$\Delta\nu_{21}(K)=F_2(K)-F_1(K)=B_v\{(2K+1)-\tfrac{1}{2}[Y(Y-4)+4(K+1)^2]^{\frac{1}{2}}-\tfrac{1}{2}[Y(Y-4)+4K^2]^{\frac{1}{2}}\}.$$

By trial it was found that $A=108$ cm^{-1} gave the solid curve in Fig. 4b in good agreement with observed points obtained from:

$$\Delta\nu_{21}(K')=Q_2(K'')-Q_1(K'')-0.056(K''+\tfrac{1}{2}),$$

the last term correcting for spin doubling in the lower state. Equally good agreement is obtained in the (1,1) band. Thus the Hill and Van Vleck relation accurately describes the behavior of the $^2\Pi$ state over a wide range of values of K.

Λ-type doubling

Holst based his conclusion that the $^2\Pi$ state was inverted on the Λ-type doubling. The values of this splitting ($\Delta\nu_{dc}$) in the (0,0) and (1,1) bands are given in Table III and plotted in Fig. 4a for the (0,0) band. The Λ-type doubling is so small that errors of measurement make it appear quite erratic (four lines are involved in computing each point). It is doubtful if any conclusion can be drawn as to the nature of the state from the behavior of the doubling, but its trend, if anything, supports our assignment. Thus the theory for regular $^2\Pi$ states indicates that $\Delta\nu_{dc}$ for the $^2\Pi_{\frac{1}{2}}$ state should be zero at the origin, then negative with increasing J, and finally rise to positive values, while for the $^2\Pi_{\frac{3}{2}}$ state $\Delta\nu_{dc}$ should rise slowly from zero at small J. The theoretical values of the Λ-type doubling constants (p and q) calculated according to Van Vleck's theory as formulated by Mulliken and Christy,[5b] were found to be considerably larger than the observed splitting requires. This is, however, the behavior of these constants for

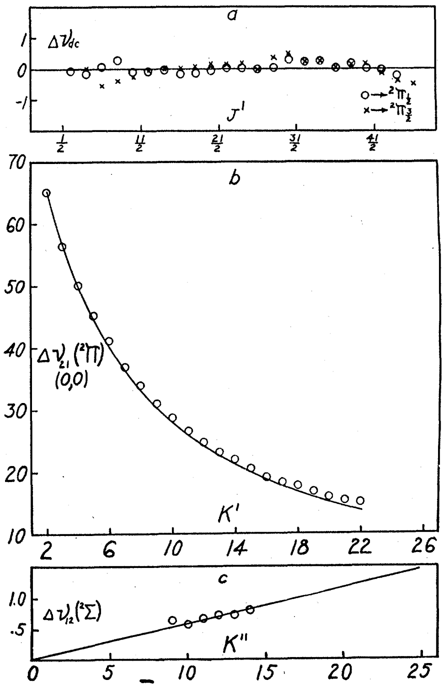

FIG. 4. (a) Λ-type doubling in $^2\Pi$ state. (b) Spin doubling in $^2\Pi$ state, (0,0) band. Observed points $Q_2(K'')-Q_1(K'')-0.056(K''+\frac{1}{2})$. Solid curve from Hill and Van Vleck formula (Eq. (1)). (c) Spin doubling in $^2\Sigma$ state. Observed points given by $^PQ_{12}(K'')-P_1(K'')$. Solid line drawn to fit observed points, equivalent to 0.056 $(K''+\frac{1}{2})$.

TABLE III. Λ-*type doubling*.
$\Delta\nu_{dc}(J+\frac{1}{2})=\frac{1}{2}[\Delta\nu_{dc}(J)+\Delta\nu_{dc}(J+1)]$.

$J+\frac{1}{2}$	(0,0) band $\Delta\nu_{1dc}(^2\Pi_{1/2})$	$\Delta\nu_{2dc}(^2\Pi_{3/2})$
1	−0.05	
2	−0.18	0.00
3	+0.09	−0.54
4	+0.28	−0.39
5	−0.10	−0.26
6	−0.05	−0.03
7	−0.05	+0.06
8	−0.18	+0.06
9	−0.13	+0.09
10	−0.02	+0.17
11	+0.05	+0.16
12	0.00	+0.16
13	−0.02	+0.06
14	+0.05	+0.38
15	+0.32	+0.50
16	+0.23	+0.29
17	+0.27	+0.24
18	+0.06	+0.14
19	+0.19	+0.16
20	+0.05	+0.20
21	−0.04	−0.08
22	−0.19	−0.38
23		−0.50
$J+\frac{1}{2}$	(1,1) band $\Delta\nu_{1dc}(^2\Pi_{1/2})$	$\Delta\nu_{2dc}(^2\Pi_{3/2})$
1	+0.09	
2	0.22	−0.25
3	0.22	0.09
4	0.14	0.06
5	0.40	0.18
6	0.69	0.22
7	0.39	−0.13
8	0.55	+0.08
9	0.47	−0.34
10	0.28	0.40
11	0.35	0.50
12	0.17	0.62
13	0.10	0.89
14		0.76

other similar molecules (for example, MgH), according to the survey made by Mulliken and Christy.[5b]

Electronic configuration. Comparison with MgH

A comparison of constants (Table IV) of AlH^+ and the "isoelectronic" molecule MgH strongly indicates that the AlH^+ system at 3632A is the analog of the well-known $^2\Pi$ (regular)$\rightarrow{}^2\Sigma^+$ system of MgH with (0,0) head at 5211A. The correspondence is evident especially in the ratio of electronic coupling coefficients in molecule and parent atom. Mulliken[6] has shown that the $\Lambda\Sigma$ coupling coefficient (A) in $^2\Pi$ molecular states is in a number of cases about nine-tenths the *ls* coupling coefficient (a) in the ^3P atomic state from which the $^2\Pi$ state is derived. It seems clear that the AlH^+ spectrum reported in this paper arises, as in MgH, from the transition $\cdots(3s\sigma)^2 3p\pi\ ^2\Pi(r) \rightarrow \cdots(3s\sigma)^2 3p\sigma\ ^2\Sigma^+$.

TABLE IV. *Comparison of AlH^+ with MgH.*

		AlH^+	MgH
$^2\Sigma$ state:	ω_e	1610 (calc.)	1494 (obs.)
	r_e	1.60A	1.73A
Spin doubling	γ	0.056	very small
$^2\Pi$ state:	ω_e	1753 (calc.)	1604 (obs.)
	r_e	1.58A	1.68A
Λ-doubling	p	~0.03	0.04
	q	very small	0.002
^3P atomic "a":	a	125.1	40.4
Molecular	A	108.	35.
A/(atomic a)		0.86	0.86
Molecular	ν_0	27,714.	19,310.
$^3P_0-{}^1S$ (atomic)		37,392. (Al II)	21,851. (Mg I)

Data for MgH from references 5b and 6. All constants (except r) in terms of cm^{-1}.

---

[6] R. S. Mulliken, Rev. Mod. Phys. **4**, 1–86 (1932).

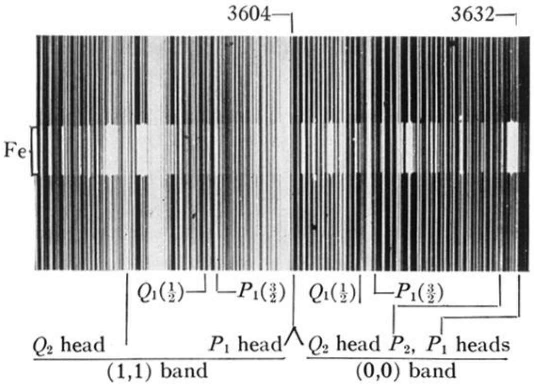

FIG. 1. Part of AlH$^+$ band system ($^2\Pi$(reg)$\rightarrow{}^2\Sigma^+$). The presence of the indicated first lines in P_1 and Q_1 branches requires that the $^2\Pi$ state be regular.